Concept of Soil Moisture Ratio for Determining the Spatial Distribution of Soil Moisture Using Physiographic Parameters of a Basin and Artificial Neural Networks (ANNs)

Edyta Kruk * and Wioletta Fudała (ID)

Department of Land Reclamation and Environmental Development, Faculty of Environmental Engineering and Land Surveying, University of Agriculture in Krakow, Al. Mickiewicza 24-28, 30-059 Kraków, Poland; wioletta.zarnowiec@urk.edu.pl
* Correspondence: edyta.kruk@urk.edu.pl

Abstract: The results of investigations on shaping the soil moisture ratio in the mountain basin of the Mątny stream located in the Gorce region, Poland, are presented. A soil moisture ratio was defined as a ratio of soil moisture in a given point in a basin to the one located in a base point located on a watershed. Investigations were carried out, using a TDR device, for 379 measuring points located in an irregular network, in the 0–25 cm soil layer. Values of the soil moisture ratio fluctuated between 0.75 and 1.85. Based on measurements, an artificial neural network (ANN) model of the MLP type was constructed, with nine neurons in the input layer, four neurons in the hidden layer and one neuron in the output layer. Input parameters influencing the soil moisture ratio were chosen based on physiographic parameters: altitude, flow direction, height a.s.l., clay content, land use, exposition, slope shape, soil hydrologic group and place on a slope. The ANN model was generated in the module data mining in the program Statistica 12. Physiographic parameters were generated using a database, digital elevation model and the program ArcGIS. The value of the network learning parameter obtained, 0.722, was satisfactory. Comparison of experimental data with values obtained using the ANN model showed a good fit; the determination coefficient was 0.581. The ANN model showed a minimal tendency to overestimate values. Global network sensitivity analysis showed that the highest influence on the wetness coefficient were provided by the parameters place on slope, exposition, and land use, while the parameters with the lowest influence were slope, clay fraction and hydrological group. The chosen physiographic parameters explained the values of the relative wetness ratio a satisfactory degree.

Keywords: soil moisture; physiographic parameters of basins; artificial neural network (ANN); redundancy analysis (RDA)

1. Introduction

Soil moisture [1,2], especially in the context of climate change, is one of the greatest problems in hydrological responses [3,4], agriculture and on industrial sites [5–9]. The question of the influence of initial soil moisture, despite being mentioned by many studies as a significant erosion factor, has rather rarely been extensively researched [10]. The actual state of soil moisture determines the beginning of surface runoff. Surface runoff is shaped by many phenomena, including exceeding a soil's full saturation and filtration possibilities, subsurface outflow, and groundwater filtration [11,12]. The spatial distribution of soil moisture is realized by various methods [13], such as: direct measurements; the use of models based on physiographic basin parameters [14] as well as remote sensing data [15,16]; and in many cases, a combination of the above methods; and has been the subject of interest of many authors.

Gómez-Plaza et al. [17] carried out investigations of moisture distribution in a small basin located in Spain, using 50 sample points over a 20 m × 20 m regular network.

They used a TDR (time domain reflectometry) device to measure the soil moisture at depths of 15 cm. They connected the spatial distribution of soil moisture with use of TWI (topographic wetness index). They also pointed out a use for these indicators for rather wet climates. TWI is calculated by the following equation:

$$TWI = ln\left(\frac{\alpha}{tan\beta}\right) \tag{1}$$

where: α is the specific catchment area defined as the local upslope area draining through a unit contour length, which is equal to the grid cell width in this study; and β is the local slope gradient [18].

Tombul [19], simulating surface runoff depending on soil initial moisture, introduced shaping of the spatial distribution in the upper soil layer. The investigations were carried out in the Kurukavak river basin, located in Turkey, in a 4.25 km^2 area. Soil moisture measurements were carried out by means of a TDR device. For investigation of spatial distribution, he used the Xinanjiang model [20], based on basic hydrological responses such as: evapotranspiration, runoff generation and flow routing, connecting soil moisture distribution with wetness index (WI):

$$\theta_{WI} = \theta_s \cdot \frac{1 - \left(1 - \frac{\theta}{\theta_s}\right)^{\frac{1}{1+b}}}{1 - (1 - WI)^{\frac{1}{b}}} \tag{2}$$

where: θ_{WI} is the critical value of capacity, θ_s is the moisture at full saturation, $\theta_{WI} \leq \theta_s$, θ is the actual moisture, b is the shape parameter.

For his investigations, he used high-resolution DEM, constructed based on a topographic map, using the vector model TIN (triangulated irregular network). The introduced distribution was substituted by a topographic index.

Zhang et al. [21] researched the spatial distribution of soil moisture at the 10-cm layer, on a 9.8-ha experimental plot, using a 15 m × 15 m network comprising 250 points in total. They showed that moisture was characterized by the normal distribution. Spatial distribution was examined using kriging, using the module Spatial Analyst connected in the program ArcGIS release 9.0. They showed the significance of investigations of moisture distribution for fertilization and irrigation needs.

Merdun et al. [22] studied the spatial distribution of water retention, for three various initial moistures (dry, mean, and wet), obtained using a rainfall simulator on soil at the experimental centre of the University of Sutcu Imam in Turkey, using 100 sampled points. The structure of the spatial distribution and the semivariogram were executed in the program GS+ 5.1.

Penna et al. [23] investigated moisture distribution in the upper soil layer, in a 1.9 km^2 area located in a mountain basin in the Italian Alps, using 42 sample points. They showed the significance of relief parameters and atmospheric conditions, including slope, TWI, exposition, and solar radiation for the shaping of this property, showing a 42% share of these factors to explain moisture distribution.

Temimi et al. [24] studied the distribution of soil moisture in the Mackenzie River basin, over a 4000 km^2 area located in Canada. In their investigations, they used a modified, not-statistical topographic wetness index (TWI), determined based on DEM:

$$TWI = ln(a) - ln(\alpha \cdot tan(\beta)) \cdot e^{-u\ LAI}) \tag{3}$$

where: a is the alimentation area, β is the local slope, LAI is the leaf area index, μ is the coefficient of radiation extinction, depending on plant cover, with values between 0.35 and 0.70.

DEM was determined in the framework of the program Shuttle Radar Topography Mission (SRTM). LAI was in turn determined from satellite observations.

Fan et al. [25] carried out investigations on spatial variability of soil moisture, using a regular 50 m network with 20 sample points, on an experimental field in China. They used kriging, realized in the program ArcGIS release 9.0.

Nikolopulos et al. [11] carried out investigations on the influence of initial soil moisture in the Fella river basin, including an area of 623 km^2 and their subbasins, located in the Italian Alps, using peak flow and outflow discharge during a rainstorm. For investigation of the spatial distribution of soil moisture, they used the hydrologic model Triangulated Irregular Network (TIN), based on the Real-Time Integrated Basin Simulator. They used a DEM with a resolution of 20 m.

Jia et al. [26] examined the temporary stability of spatial distribution of moisture in loess soil in China, on five experimental plots of dimension 61 × 5 m, in 10 cm intervals, up to a depth of 1 m. They showed that the vertical distribution of moisture does not have a unitary trend; however, the horizontal distribution was similar for the same layers, irrespective of a density increase.

This work aims to present the concept of determination of soil moisture distribution, based on physiographic parameters of a basin, realized by the use of artificial neural networks (ANNs).

2. Materials and Methods

2.1. Study Sites

The study was carried out in the Outer Western Carpathians, in the southern region of Małopolska Province, Poland (Figure 1). The Mątny Stream (1.47 km^2) flows into the Mszanka River in the hamlet of Skiby at 20°9′2.35″ E, 49°37′30.52″ N. The main watercourse starts at 20°08′28.52″ E, 49°36′25.44″ N. The mean annual air temperature is 7.4 °C. The lowest temperature of −25.8 °C was recorded on 3 February 2012 and the highest, 33.0 °C, on 8 July 2013. The long-term annual average total precipitation is 846.63 mm and the total precipitation over the years in the study was 948.1 mm. The highest daily precipitation was 100.7 mm on 15 May 2014. The snow usually starts to melt at the beginning of March. The growing season starts around 10 April, and the winter begins around 30 November.


Map of Poland   Location of the investigation area
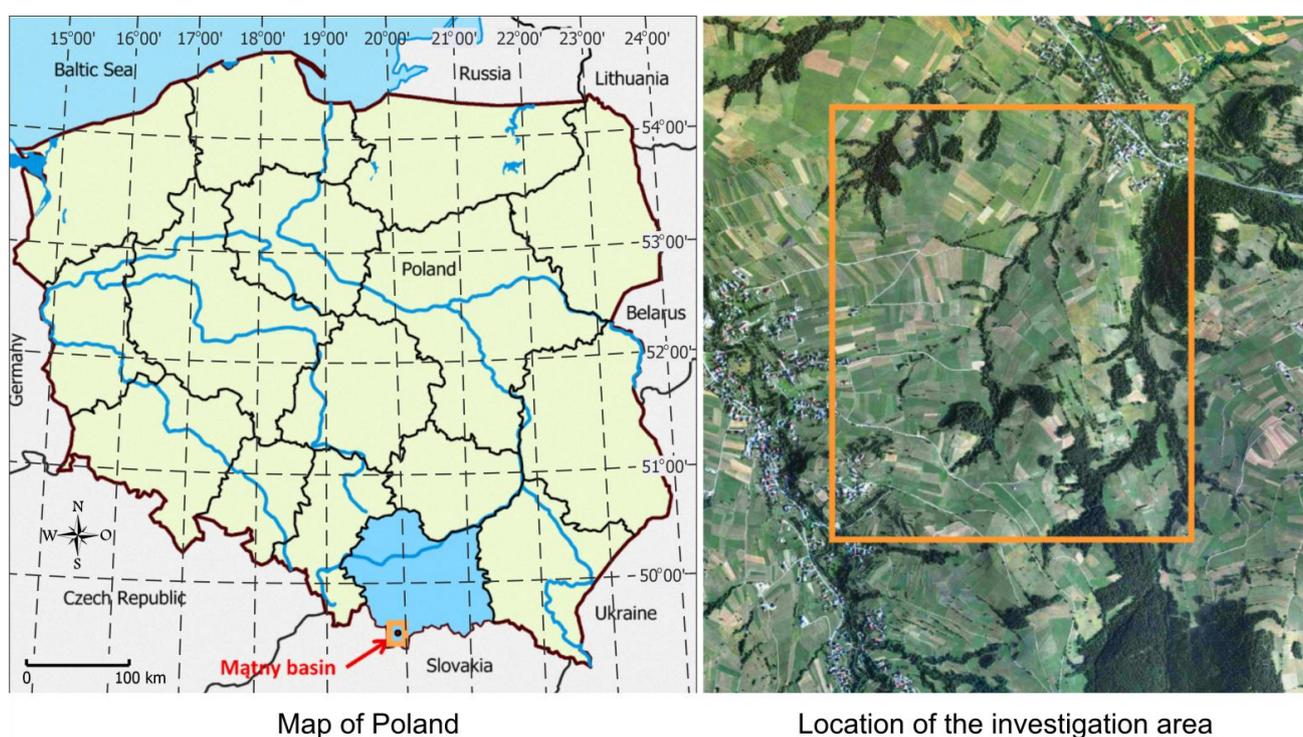
Figure 1. Location of the research area within Poland.

The terrain comprises low- and medium-height mountains with peak heights ranging from 617.6 m above sea level (m.a.s.l.) to 732.0 m.a.s.l. The lowest point is situated 490.0 m.a.s.l. The mean height of the catchment is 582.66 m.a.s.l. [27]. The slope distribution is as follows: <5%, (0.06 km^2); 5–10% (0.27 km^2); 10–18% (0.67 km^2); 18–27% (0.31 km^2); and >27% (0.16 km^2). The weighted average slope for the entire catchment was 16.28% [28]. The catchment land use structure was dominated by grassland (73.5%); arable lands constituted 14.3% and included the following crops: spring oats (*Avelana sativa*), 7.3%; potatoes (*Solanum tuberosum*), 4.3%; and common wheat (*Triticum aestivum*), 2.7%. Forests accounted for 9.5% and urban areas for 2.7% of the catchment land (Figure 2). The catchment area is cut by a network of dirt roads. Most of them are deeply furrowed and tend to transform into water-carrying streams during and after rain events.


Figure 2. Photos showing typical land use of the Mątny basin.

Soils in the catchment area are diverse, depending on slope location. The soil cover in the Mątny stream catchment is dominated by loamy soils, including sandy clay loam, loam, silt loam, clay loam and sandy loam. Pedological conditions were identified by analysis of a 1:25,000 agricultural soil map and categorized into the respective groups according to USDA standards [29].

2.2. Experimental Design/Models Applied

Calculations implementing the soil moisture ratio (wetness coefficient) model algorithm were performed using the interface of ArcGIS 10.3.1 software [30]. The spatial data were obtained based on the Polish State Surveying Coordinate System (PUGW). The following parameters were determined: altitude, slope, flow direction, exposition, shape of the slope, situation on the slope, hydrological group, use, and clay fraction. Thematic layers were developed using the sources specified in Table 1.

Table 1. Description of parameters used in coefficient wetness model.

Parameter	Explanation	
DEM	Geodesic and Cartographic Documentation Centre	Scale 1:5000, resolution 5 m
Altitude	meters mean sea level	m.a.s.l.
Slope	Differences of heights between the points Δh divided by length of projection of direction between the points, l; [%] [1]	Intervals, %:0–5; 5–10; 10–18; 18–27; >27
Flow direction	Determined based on height difference between the given cell determined each of the eight adjacent cells, based on one-direction points model D8 [2] [31], where: Z is the number of adjacent cells, h is the resolution of the GRID model, hØ(i) is the distance between the middle points of cell, 1 for the ones situated in the cardinal directions (N,E,S,W), root square for the two remaining ones.	Convention of the DEM numbering (a) in standard cell system, (b) in determination of flow directions, (c) coding of flow directions by the D8 algorithm [31]
Exposition	Location on the slope with respect to the direction of sunlight rays, determined using a 4-grade scale, as one of the geographical directions.	East–E, west–W, north–N, south–S
Shape of the slope	Concave, flat, convex	
Situation on a slope	Determined using a five-grade scale: hilltop, slope outset, slope middle, slope bottom, slope foot	Place on slope: 1- hilltop 2- slope outset 3- slope middle 4- slope bottom 5- slope foot
Digital soil map	Institute of Soil Science and Plant Cultivation State Research Institute	Scale 1:25,000
Hydrological soil group	Determined based on U.S. Department of Agriculture–Natural Resources Conservation Service [32] method	Groups:A, B, C, D
Use	Orthophoto map; site inspection	Scale 1:1000Data: 25.07.2014
Clay fraction	Determined using the Casagrande'a method. Soil samples were collected from a top layer of the soil (0 to 10 cm) in 43 selected study plots.	
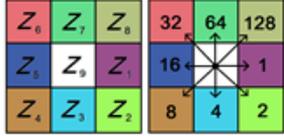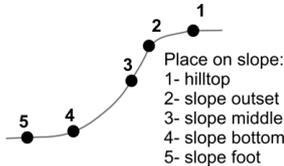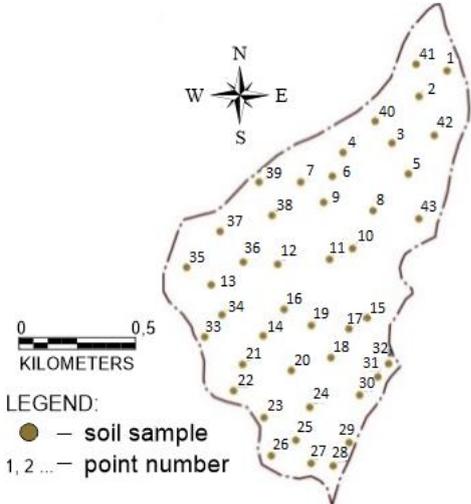
where: [1] is $S = \frac{\Delta h}{l} \cdot 100$; [2] is $S_{D8} = max_{i=1,8} \frac{Z_9 - Z_i}{h\varnothing(i)}$.

Three sampling time periods were adopted for each of the three growing seasons: dry (period I), medium (period II) and wet (period III) AMC (Antedescent Moisture Conditions), distinguished based on the sum of rainfall from the previous 5 days (mm) and the season category (dormant or growing) (Table 2). In botany and agriculture, the growing season is defined as the portion of each year when native plants and ornamental plants grow, while the dormant season is when growth and development are temporarily stopped [33]. In much of Europe, the growing season is defined as the average number of days with a 24-h average temperature of at least 6 °C; in southern Poland, this typically lasts from April to September.

Table 2. AMC classes [34].

AMC Classes	Vegetative Dormant Season	Vegetative Growing Season
I	Less than 12.7	Less than 35.5
II	12.7 to 28.0	35.5 to 53.3
III	More than 28	More than 53.3

The soil moisture ratio $K_{w,i}$ in point i was determined based on the concept of wetness coefficient [35,36]:

$$K_{w,i} = \frac{\theta_i}{\theta_b} \tag{4}$$

where: θ_i is the soil volumetric water in the given point i within the basin area [m$^3 \cdot$m^{-3}], and θ_b is the soil volumetric water content in the basal point [m$^3 \cdot$m^{-3}].

From this, the soil moisture in a point i in a basin can by determined as:

$$\theta_i = \theta_b \cdot K_{w,i}(p_1,\ p_2 \ldots p_n) \tag{5}$$

where: $K_{w,i}(p_1,\ p_2\ \ldots\ p_n)$ is the relative wetness coefficient determined based on the following parameters: place on a slope, exposition, land use, shape of slope, altitude, flow direction, slope, clay fraction, hydrological group.

The purpose of the wetness coefficient was to assess the distribution of soil moisture in the catchment area, based on the measurement from a basal point located on a hilltop. Soil moisture was measured in 2014, between 11:00 pm and 14:00 am during days without and with rainfall using the TDR device, as a mean value in the 0–0.10 m layer, for 379 measuring points (153 for period I, 100 for period II and 126 for period III). The distribution of points was random, taking into account the specific character of the mountain catchment. The measurements were made, for period I, on 25 July (the sum of rainfall from the previous 5 days was 21.2 mm, in the vegetative growing season); for period II, on 4 October (the sum of rainfall from the previous 5 days was 21.7 mm, in the growing season); and for period III, on 25 September (the sum of rainfall from the previous 5 days was 34.8 mm, in the dormant season) (Figure 3).
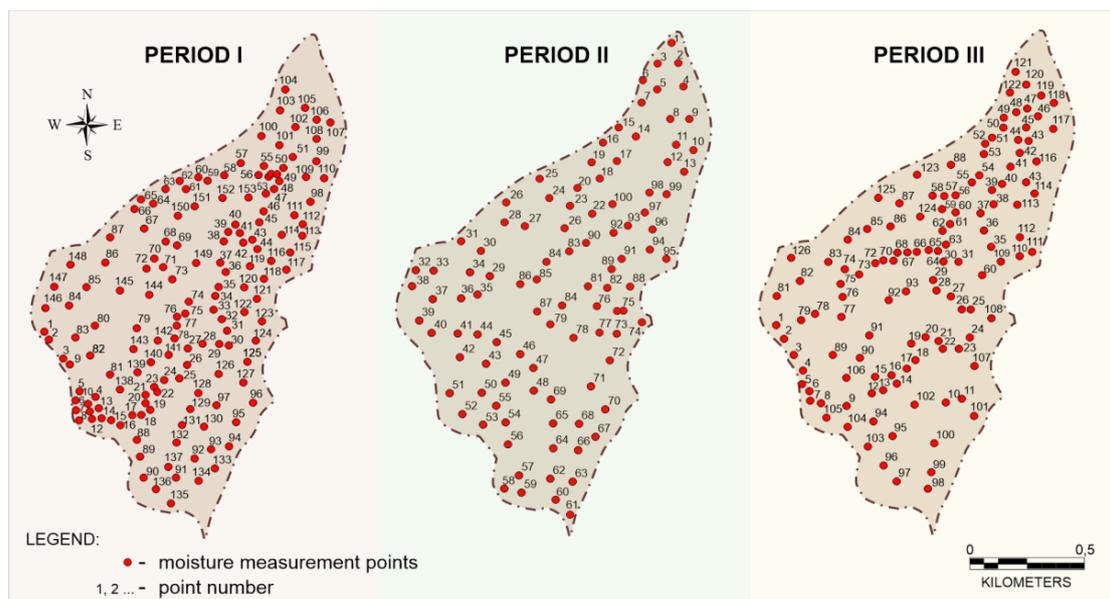
Figure 3. Location of moisture measurement points.

2.3. Statistical Analysis and Data Procedure

An ANN (artificial neural network) model in the form of a multilayer perceptron (MLP) was used to generate wetness coefficients, using Statistica software (release 12.5). A total of 70% of all variables were applied for the learning process; 15% were used for validation and 15% to test the model. A quasi-Newton algorithm with a Broyden–Fletcher–Goldfarb–Shanno (BFGS) modification was selected for the learning neural network. The sum of squares (SOS) was treated as the error function. The artificial neural network model was used to establish the association between the wetness coefficient, whereas a physiographic parameter, indicative of the soil and its use, was applied in all data set as an independent variable. The multi-layer perceptron consisted of three layers of neurons: (1) an input layer, (2) an output layer and (3) intermediate (hidden) layers. Each neuron had a number of inputs (from outside to the subsequent layer or out of the network) [37]. In this study, the network system included an input and a hidden layer made of nine neurons (altitude, slope, flow direction, exposition, shape of the slope, situation on a slope, hydrological group, land use and clay fraction) and an output layer with one neuron (wetness coefficient).

Studies on the percentage effect of selected soil, use and physiographic parameters were carried out using ANN based on a global network sensitivity analysis [38–40].

RDA (redundancy analysis) of standardized environmental variables was performed to explain and describe the pattern of variability in a parameter [41] Multivariate analysis showed the presence of two main gradients of environmental variables. Positions of the vectors of independent variables were proportional to the loading factors. The multivariate analysis was carried out with Canoco for Windows version 4.51.

The analysis of empirical model adjustment to experimental data was carried out using the following metrics [42], presented in Table 3.

Table 3. Measures of model performance [43,44].

Measure	Equation
Mean error of prediction	MEP [1]
Root mean square error	RMSE [2]
Mean percentage error	MPE [3]
Model efficiency	ME [4]

where: [1] is $MEP = \frac{1}{n} \cdot \sum_{i=1}^{n} \left(c_i^m - c_i^p \right)$; [2] is $RMSE = \sqrt{\frac{1}{n} \cdot \sum_{i=1}^{n} \left(c_i^m - c_i^p \right)^2}$; [3] is $MPE = \frac{1}{n} \cdot \sum_{i=1}^{n} \frac{c_i^m - c_i^p}{c_i^m} \cdot 100\%$; [4] is $ME = 1 - \frac{\sum_{i=n}^{n} \left(c_i^m - c_i^p \right)^2}{\sum_{i-n}^{n} \left(c_i^m - \bar{c} \right)^2}$; c_i^m is the measured values, c_i^p is the computed values, and n is the number of data.

Spatial variability of the investigated and measured values of the soil moisture ratio was determined using kriging. The kriging method allows to obtain the most probable values in any part of an investigated area and to find the location for new measuring points. To briefly define the technique of kriging, it is a method for optimizing the estimation of the spatially correlated quantity Z, both in stationarity and non-stationarity instances.

3. Results

Moisture at the base point was 0.146 m^3·m^{-3} in the dry season (period I), 0.247 m^3·m^{-3} in the medium season (period II), and 0.433 m^3·m^{-3} in the wet season (period III). The measured moisture fluctuated between 0.086 m^3·m^{-3} and 0.226 m^3·m^{-3} for period I, between 0.146 m^3·m^{-3} and 0.354 m^3·m^{-3} for period II, and between 0.145 m^3·m^{-3} and 0.441 m^3·m^{-3} for period III. The obtained values were in accordance with the ones introduced in the literature [45] The ANN model was then generated based on the results of the investigation of physiographic parameters (Figure 4).
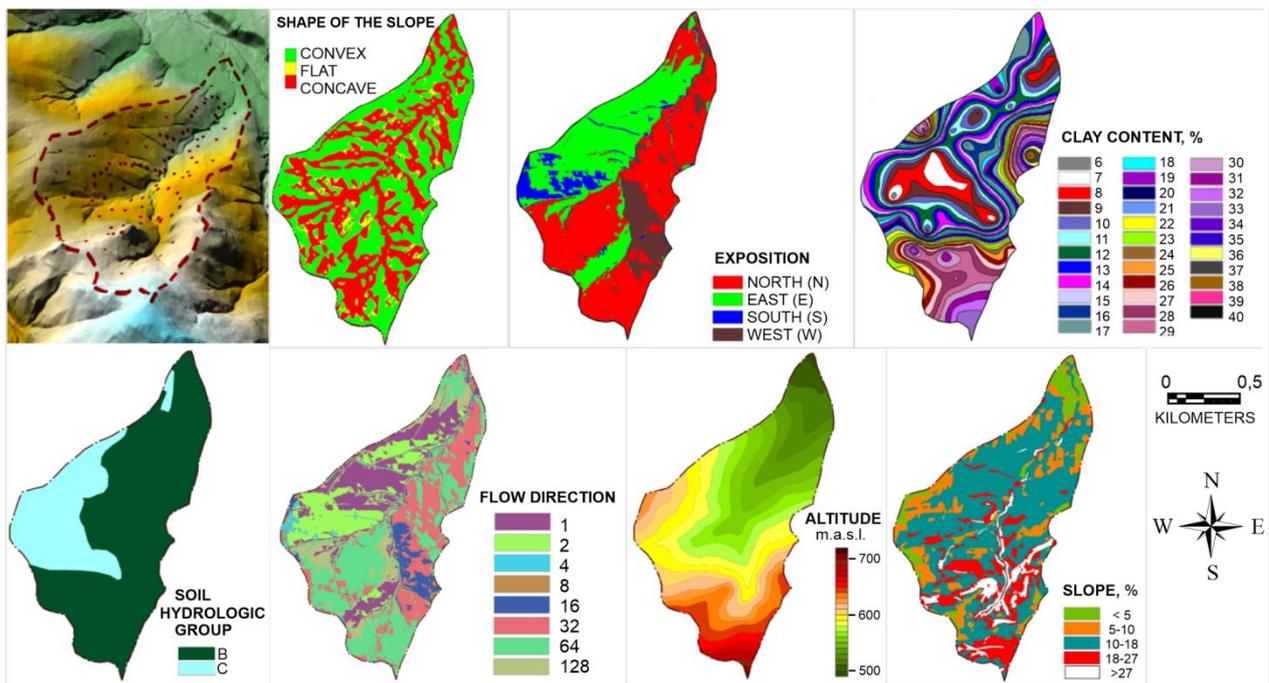
Figure 4. Physiographical parameters of the Mątny stream basin.

The best-fitting model turned out to be the MLP 9-4-1, with four perceptrons in the hidden layer. The MLP 9-4-1 model is characterized by high fitting quality and low error, and therefore presents a good adjustment (Table 4). Thanks to the global sensitivity analysis (Table 5), the relative and absolute influence of a number of parameters on the soil moisture ratio K_w were determined.

Table 4. Analysis of quality and errors of the MLP 9-4-1.

Quality	learning	0.757
	testing	0.752
	validation	0.807
Error	learning	0.006
	testing	0.009
	validation	0.004
Perceptron activation functions	hidden	
	output	

Table 5. Global sensitivity analysis of the MLP 9-4-1 model.

No.	Parameter	Relative Sensitivity	Absolute Influence [%]
1	Place on slope	11.3	40
2	Exposition	3.5	12
3	Use	3.0	11
4	Shape of the slope	2.9	10
5	Altitude	2.9	10
6	Flow direction	1.6	5.0
7	Slope	1.3	5.0
8	Clay fraction	1.0	4
9	Hydrological group	1,0	4

In the Mątny stream basin, the parameters place on the slope (40%) and exposition (12%) had the highest impact (Table 5). Values of the soil moisture ratio fluctuated between 0.75 and 1.85. Based on the simulated values of the soil moisture ratio for every one of the measured points, the map of the spatial distribution of this parameter was generated using Surfer 10 and ArcGIS, based on data generated by ANN 9-4-1 (Figure 5a) and on the measurement date (Figure 5b). The highest values of the soil moisture ratio occurred in the northwest part of the basin. Figure 6 presents a comparison between the ANN simulated values of the soil moisture ratio and the one elaborated based on measured data. Values of the simulated wetness coefficient ranged between 0.89 and 1.13. Model efficiency measures for the MLP 9-4-1 were as follows: MEP: 0.004, RMSE: 0.104, MPE: −0.6%, ME: 0.580 and R^2: 0.581 (Table 6).
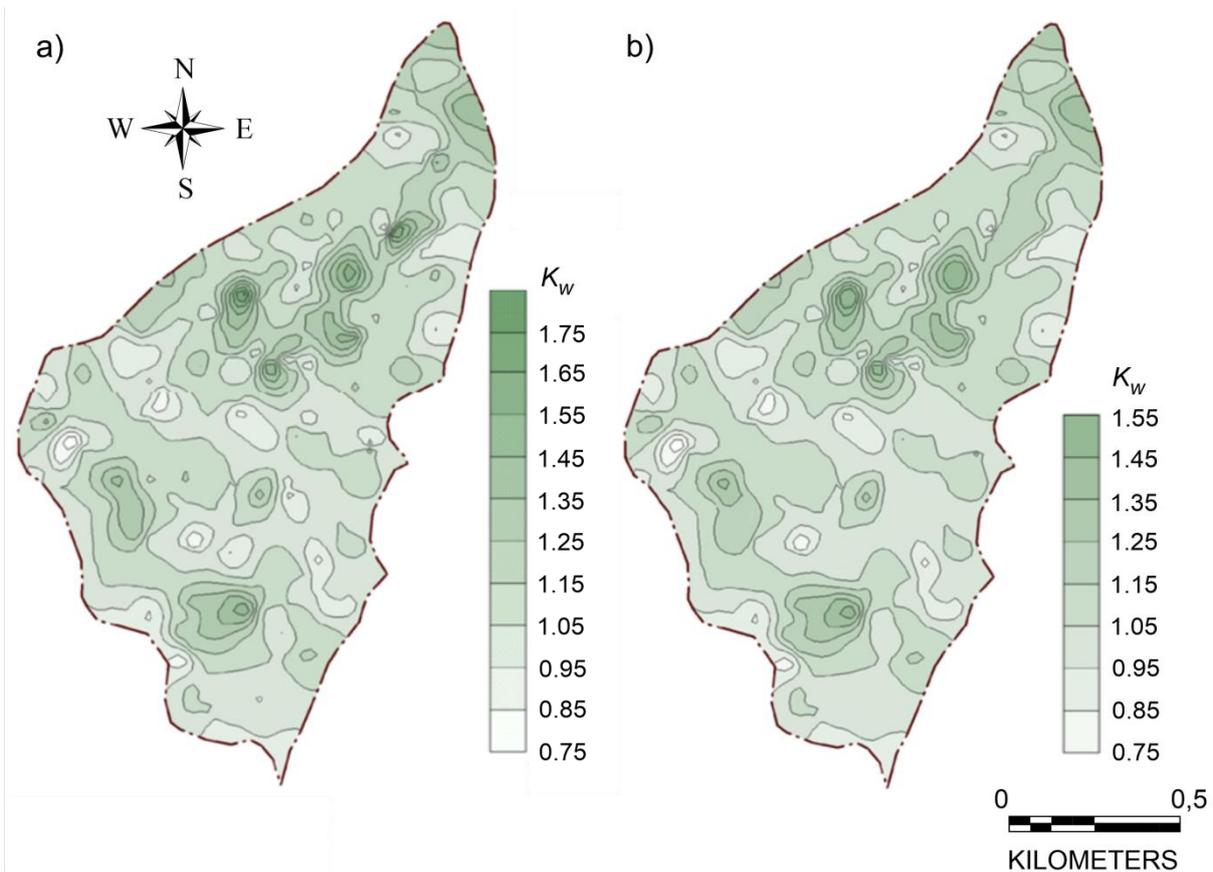

Figure 5. Spatial distribution of the soil moisture ratio in the Mątny basin generated using: (**a**) the MLP 9-4-1 model, and (**b**) based on measured data elaborated by kriging technique.

Table 6. Model efficiency measures for the MLP 9-4-1.

| Model Efficiency Measures.				
MEP	RMSE	MPE [%]	ME [-]	R^2 [-]
0.004	0.104	−0.6	0.580	0.581
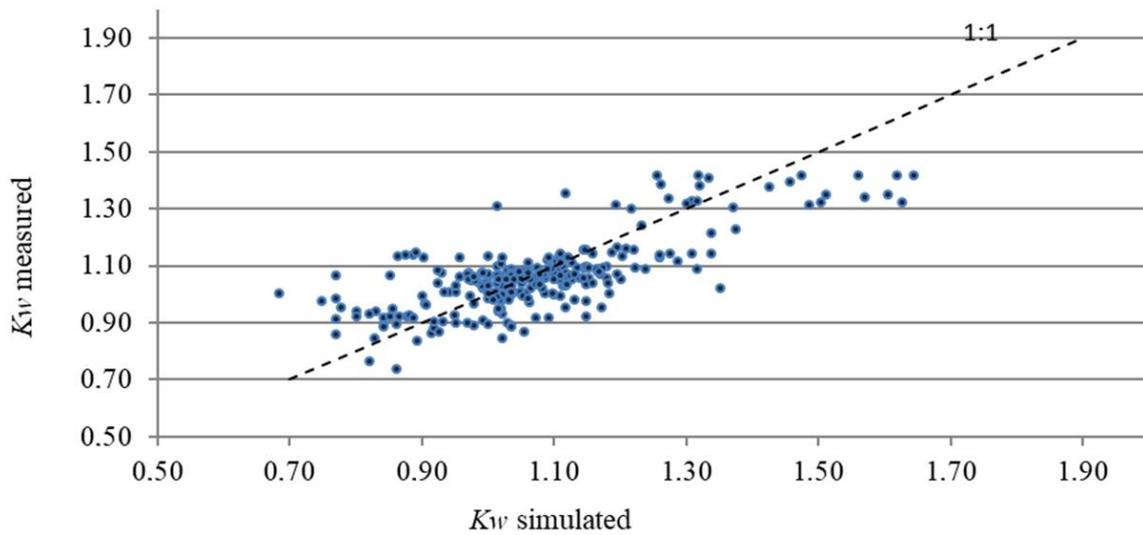
Figure 6. The measured versus simulated soil moisture ratio.

Multivariate analysis (RDA) was employed to explain the relative importance of particular explanatory variables and underline differences between parameters. The patterns of the independent variables for soil factors and environmental parameters are shown on the plot (Figure 7). We noted a positive correlation among the flow direction, slope, clay content and wetness coefficient. Generally, multivariate analysis for the studied parameters indicated a strong positive correlation among the soil hydrologic group. Moreover, we saw a correlation between altitude and place on the slope. On the other hand, only exposition N, exposition E and exposition W were strongly negatively correlated to other examined parameters. The first component described 27.43% of the total variation, and the second component explained 42.01% of the total variance among the study parameters.
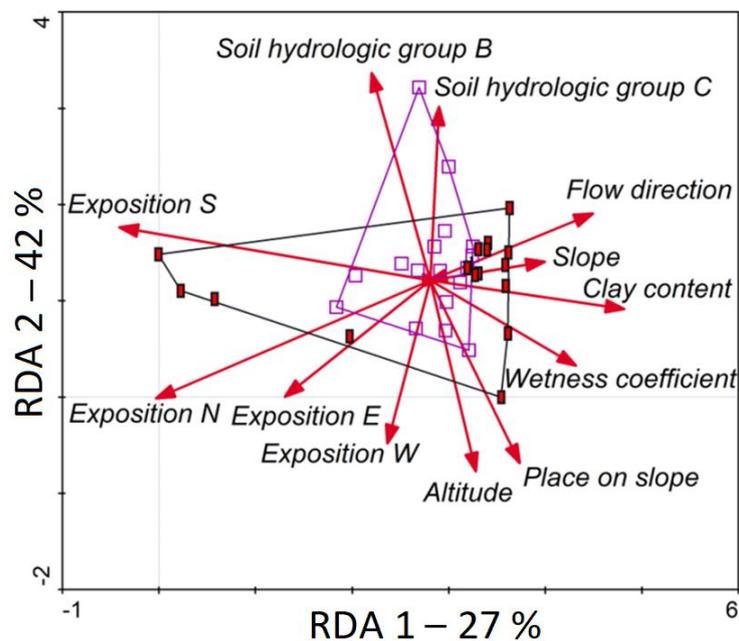

Figure 7. Multivariate RDA analysis for the soil moisture ratio is created by vectors (red squares are for convex; purple squares for concave slopes).

4. Discussion

In this study, the concept of relative wetness coefficient was developed as a base for determination of the spatial distribution of soil moisture on an area of a mountain basin.

The idea of the coefficient is based on the observations that there is a relation between soil moisture in a point on a slope and on a flat in a basin. Values of relative wetness coefficient were obtained by the ANN model generated based on nine basin parameters: place on a slope, exposition, land use, shape of slope, altitude, flow direction, slope, clay fraction and hydrological group and direct measurements of soil moisture on the area of small Carpathian basin (1.47 km^2). Parameters of ANN learning, testing, validation, and model efficiency measures were very satisfactory. The model overestimated prognosed values only of 0.6%. Model was fitted to the experimental data very well. Based on the ANN model, the sequence of significance of the particular basin parameters were arranged to provide the relative wetness coefficient explanation. The highest influence had: place on slope, exposition, and land use. In turn, clay fraction and the hydrological group had no significance, because the investigated basin is not highly differentiated regarding soil. A very interesting model for evaluation of the relative wetness coefficient foe small basin was presented by Svetlitchnyi et al. [33]. It was based on basin parameters such as: the shape of slope, distance from the divide, slope aspect and overall length of a slope. The obtained model errors were very satisfactory. The relative wetness coefficient can be used as an easy way to determine the distribution of soil moisture in the upper layer in small mountain basins.

5. Conclusions

The soil moisture ratio, as a relation between soil moisture in a given point and in a basal point located on a flat, generated based on basin parameters, by use of artificial neural networks is one of the simplest ways to determine the distribution of soil moisture on an area of small mountain basin. The main basin parameters that can influence the relative soil moisture ratio are the place on a slope, exposition, land use (if it is not uniform on an area of a basin), shape of slope and altitude. Our investigations showed that they controlled the relative soil moisture ratio in sum in 83%. The model for determination of the relative soil moisture ratio, generated by use of the ANN, gave very satisfied results in terms of errors, and explained as many as 58% of cases. The ANN model overestimated prognosis values only of 0.6%. For larger basins and basins with highly differentiated soil, the next studies have to be carried out.

Author Contributions: Conceptualization, E.K. and W.F.; methodology, E.K.; software, E.K.; validation, E.K. and W.F.; formal analysis, E.K.; investigation, E.K. and W.F.; resources, E.K. and W.F.; data curation, E.K. and W.F.; writing—original draft preparation, E.K.; writing—review and editing, E.K. and W.F.; visualization, E.K. and W.F.; supervision, E.K.; project administration, E.K.; funding acquisition, E.K. and W.F. Both authors have read and agreed to the published version of the manuscript.

Institutional Review Board Statement: Not applicable.

Informed Consent Statement: Not applicable.

Data Availability Statement: Not applicable.

Conflicts of Interest: The authors declare no conflict of interest.

References

1. Li, J.; Islam, S. Estimation of root zone soil moisture and surface fluxes partitioning using near surface soil moisture measurement. *J. Hydrol.* **2002**, *259*, 1–14. [CrossRef]
2. Romana, N. Soil moisture at local scale: Measurements and simulations. *J. Hydrol.* **2014**, *516*, 6–20. [CrossRef]
3. Castillo, V.M.; Gómez-Plaza, A.; Martinez-Mena, M. The role of antecendent soil water content in the runoff response of a semiarid catchment: A simulation approach. *J. Hydrol.* **2003**, *284*, 114–130. [CrossRef]
4. Western, A.W.; Zhou, S.L.; Grayson, R.B.; McMahon, T.A.; Blöschl, G.; Wilson, D.J. Spatial correlation of soil moisture in small catchments and its relationship to dominant spatial hydrological processes. *J. Hydrol.* **2004**, *286*, 113–134. [CrossRef]

5. Boroń, K.; Klatka, S.; Ryczek, M.; Liszka, P. Kształtowanie się właściwości fizycznych, fizykochemicznych i wodnych rekulty-wowanego i niezrekultywowanego osadnika byłych Krakowskich Zakładów Sodowych "Solvay"/The formation of the physical, physico-chemical and water properties reclaimed and not reclaimed sediment reservoir of the former Cracow Soda Plant "Solvay". *Acta Sci. Pol. Form. Circumiectus* **2016**, *15*, 35–43. [CrossRef]

6. Brocca, L.; Morbidelli, R.; Melone, F.; Moramarco, T. Soil moisture spatial variability in experimental areas of central Italy. *J. Hydrol.* **2007**, *333*, 356–373. [CrossRef]

7. Klatka, S.; Malec, M.; Ryczek, M.; Boroń, K. Wpływ działalności eksploatacyjnej Kopalni Węgla Kamiennego "Ruch Borynia" na gospodarkę wodną wybranych gleb obszaru górniczego/Influence of mine activity of the coal mine "Ruch Borynia" on water management of chosen soils on mining area. *Acta Sci. Pol. Form. Circumiectus* **2015**, *14*, 115–125. Available online: http://www.formatiocircumiectus.actapol.net/tom14/zeszyt1/14_1_115.pdf (accessed on 24 February 2021). [CrossRef]

8. Klatka, S.; Malec, M.; Ryczek, M.; Kruk, E.; Zając, E. Ocena zdolności retencyjnych wybranych odpadów przemysłowych/ Evaluation of retention ability of chosen industrial wastes. *Acta Sci. Pol. Form. Circumiectus* **2016**, *15*, 53–60. Available online: http://www.formatiocircumiectus.actapol.net/tom15/zeszyt4/15_4_53.pdf (accessed on 15 January 2021).

9. Wei, J.B.; Xiao, D.N.; Zeng, H.; Fu, Y.K. Spatial variability of soil properties in relation to land use and topography in a typical small watershed of the black soil region, northeastern China. *Environ. Geol.* **2008**, *53*, 1663–1672. [CrossRef]

10. Boron, K.; Klatka, S.; Ryczek, M.; Zając, E. Reclamation and cultivation of the Cracow soda plant lagoons, International Conference on Construction for a Sustainable Environment, Vilnius, LITHUANIA, JUL 01–04, 2008. In *Construction for a Sustainable Environment*, 1st ed.; Sarsby, R., Ed.; Routledge: London, UK, 2010; pp. 245–250. Available online: https://www.routledge.com/Construction-for-a-Sustainable-Environment/Sarsby-Meggyes/p/book/9780415566179 (accessed on 20 July 2021).

11. Nikolopulos, E.I.; Anagnostou, E.N.; Borga, M.; Vivoni, E.R.; Papadopoulos, A. Sensitivity of a mountain basin flash flood to initial wetness condition and rainfall variability. *J. Hydrol.* **2011**, *402*, 165–178. [CrossRef]

12. Santra, P.; Sankar, B.; Chakravarty, D. Spatial prediction of soil properties in a watershed scale through maximum likelihood approach. *Environ. Earth Sci.* **2012**, *65*, 2051–2061. [CrossRef]

13. Alvarez-Garreton, C.; Ryu, D.; Western, A.W.; Crow, W.T.; Robertson, D.E. The impacts of assimilating satellite soil moisture into a rainfall-runoff model in a semi-arid catchment. *J. Hydrol.* **2014**, *519*, 2763–2773. [CrossRef]

14. Kruk, E.; Klapa, P.; Ryczek, M.; Ostrowski, K. Influence of DEM Elaboration Methods on the USLE Model Topographical Factor Parameter on Steep Slopes. *Remote Sens.* **2020**, *12*, 3540. [CrossRef]

15. Tischler, M.; Garcia, M.; Peters-Lidard, C.; Moran, M.S.; Miller, S.; Kumar, S.; Geiger, J. A GIS framework for surface-layer soil moisture estimation combining satellite radar measurements and land surface modeling with soil physical property estimation. *Environ. Model. Softw.* **2007**, *22*, 891–898. [CrossRef]

16. Vidhya Lakshmi, S.; Jijo, J.; Soundariya, S.; Vishalini, T.; Kasinatha Pandian, P. A comparison of Soil Texture Distribution and Soil Moisture Mapping of Chennai Coast using Landsat ETM+ and IKONOS Data. CONFERENCE ON WATER RESOURCES, COASTAL AND OCEAN ENGINEERING (ICWRCOE 2015). *Aquat. Procedia* **2015**, *4*, 1452–1460. [CrossRef]

17. Gómez-Plaza, A.; Martinez-Mena, M.; Albaladejo, J.; Castillo, V.M. Factors regulating spatial distribution of soil water content in small semiarid catchments. *J. Hydrol.* **2001**, *253*, 211–226. [CrossRef]

18. Zhao, L.; Liu, Y.; Luo, Y. Assessing Hydrological Connectivity Mitigated by Reservoirs, Vegetation Cover, and Climate in Yan River Watershed on the Loess Plateau, China: The Network Approach. *Water* **2020**, *12*, 1742. [CrossRef]

19. Tombul, M. Mapping Field Surface Soil Moisture for Hydrological Modeling. *Water Resour. Manag.* **2007**, *21*, 1865–1880. [CrossRef]

20. Gou, W.; Wang, C.; Ma, T.; Zeng, X.; Yang, H. A distributed Grid-Xinanjiang model with integration of subgrid variability of soil storage capacity. *Water Sci. Eng.* **2016**, *9*, 97–105.

21. Zhang, C.; Liu, S.; Fang, J.; Tan, K. Research on the spatial variability of soil moisture based on GIS. In *Computer and Computing Technologies in Agriculture, Volume I, The International Federation for Information Processing, Vol. 258, Proceedings of the First IFIP TC 12 International Conference on Computer and Computing Technologies in Agriculture (CCTA 2007), Wuyishan, China, 18–20 August 2007*; Li, D., Ed.; Springer: Boston, MA, USA, 2008; pp. 719–727. [CrossRef]

22. Merdun, H.; Meral, R.; Riza Demirkiran, A. Effect of the initial soil moisture content on the spatial distribution of the water retention. *Eurasian Soil Sci.* **2008**, *41*, 1098–1106. [CrossRef]

23. Penna, D.; Borga, M.; Norbiato, D.; Dalla Fontana, G. Hillslope scale soil moisture variability in a steep alpine terrain. *J. Hydrol.* **2009**, *364*, 311–327. [CrossRef]

24. Temimi, M.; Leconte, R.; Chaouch, N.; Sukumal, P.; Khanbilvardi, R.; Brissette, F. A combination of remote sensing data and topographic attributes for the spatial and temporal monitoring of soil wetness. *J. Hydrol.* **2010**, *388*, 28–40. [CrossRef]

25. Fan, Y.; Zhang, C.; Fang, J.; Tian, L. Research on Regional Spatial Variability of Soil Moisture Based on GIS. In *Computer and Computing Technologies in Agriculture III, IFIP Advances in Information and Communication Technology, Proceedings of the Third IFIP TC 12 International Conference (CCTA 2009), Beijing, China, 14–17 October 2009*; Li, D., Zhao, C., Eds.; Springer: Berlin/Heidelberg, Germany, 2010; Volume 317, pp. 466–470. [CrossRef]

26. Jia, Y.H.; Shao, M.A.; Jia, X.X. Spatial pattern of soil moisture and its temporal stability within profiles on a loessial slope in northwestern China. *J. Hydrol.* **2013**, *495*, 150–161. [CrossRef]

27. Halecki, W.; Kruk, E.; Ryczek, M. Loss of topsoil and soil erosion by water in agricultural areas: A multi-criteria approach for various land use scenarios in the Western Carpathians using a SWAT model. *Land Use Policy* **2018**, *73*, 363–372. [CrossRef]

28. Halecki, W.; Kruk, E.; Ryczek, M. Evaluation of Soil Erosion in the Mątny Stream Catchment in the West Carpathians Using the G2 model. *Catena* **2018**, *164*, 116–124. [CrossRef]

29. Soil Survey Staff. *Soil Taxonomy*; USDA: Washington, DC, USA, 1975; pp. 17–754.

30. Hillier, A. Manual for Working with ArcGIS10. Unpublished Paper. Available online: http://works.bepress.com/amy_hillier/24/ (accessed on 13 December 2020).

31. Wilson, D.J.; Gallant, J.C. Digital terrain analysis. In *Terrain Analysis: Principles and Applications*; Wilson, D.J., Gallant, J.C., Eds.; John Willey & Sons, Inc.: New York, NY, USA, 2000; pp. 1–27.

32. USDA—Natural Resources Conservation Service. *National Soil Survey Handbook, Title 430-VI*; US Department of Agriculture, Natural Resources Conservation Service: Washington, DC, USA, 2002.

33. Silveira, M.C.F.; Oliveira, E.M.M.; Carvajal, E.; Bon, E.P.S. Nitrogen regulation of Saccharomyces cerevisiae invertase. Role of the URE2 gene. *Appl. Biochem. Biotechnol.* **2000**, *84–86*, 247–254. [CrossRef]

34. United States Department of Agriculture. Soil Conservation Service 1993. In *National Engineering Handbook*; Section 4, Hydrolohy; Washington, DC, USA. Available online: https://directives.sc.egov.usda.gov/OpenNonWebContent.aspx?content=43924.wba (accessed on 20 July 2021).

35. Svetlitchnyi, A.A.; Plotnitskiy, S.V.; Stepovaya, O.Y. Spatial distribution of soil moisture content within catchments and its modelling on the basis of topographic data. *J. Hydrol.* **2003**, *277*, 50–60. [CrossRef]

36. Kruk, E.; Ryczek, M.; Malec, M.; Klatka, S. Kształtowanie się współczynnika wilgotności gleby w zlewni potoku Mątny w Gorcach/Shaping of the wetness coefficient in the Mątny stream basin in the Gorce mountains. *Inżynieria Ekologiczna* **2016**, *50*, 99–105. [CrossRef]

37. Dawson, J.F.; Richter, A.W. Probing three-way interactions in moderated multiple regression: Development and application of a slope difference test. *J. Appl. Psychol.* **2006**, *91*, 917–926. [CrossRef]

38. Rajurkar, M.P.; Kothyari, U.C.; Chaube, U.C. Artificial neural networks for daily rainfall-runoff modelling. *Hydrol. Sci. J.* **2002**, *47*, 865–877. [CrossRef]

39. Caamaño, D.; Googwin, P.; Manic, M. Derivation of a bedload sediment transport formula using artificial neural networks. In Proceedings of the 7th International Conference on Hydroinformatics HIC, Nice, France, 4–8 September 2006; pp. 1–8.

40. Kentel, E. Estimation of river flow by artificial neural networks and identification of input vectors susceptible to producing unreliable flow estimates. *J. Hydrol.* **2009**, *375*, 481–488. [CrossRef]

41. Lepš, J.; Smilauer, P. *Multivariate Analysis of Ecological Data Using CANOCO*; Cambridge University Press: Cambridge, UK, 2003. [CrossRef]

42. Rahnama, M.B.; Barani, G.A. Application of rainfall-runoff models to Zard River catchments. *Am. J. Environ. Sci.* **2005**, *1*, 86–89. [CrossRef]

43. Nash, J.E.; Sutcliffe, J.V. River flow forecasting through conceptual models. Part I—A discussion of principles. *J. Hydrol.* **1970**, *10*, 282–290. [CrossRef]

44. Tiwari, A.K.; Risse, L.M.; Nearing, M.A. Evaluation of WEPP and its comparison with USLE and RUSLE. *Trans. ASAE* **2000**, *43*, 1129–1135. [CrossRef]

45. Gebregiorgis, M.F.; Savage, M.J. Field, laboratory and estimated soil-water content limits. *Water SA* **2006**, *32*, 155–162. [CrossRef]